


RESEARCH

Open Access



# Deciphering the omicron variant: integrated omics analysis reveals critical biomarkers and pathophysiological pathways

Qianyue Yang<sup>1†</sup>, Zhiwei Lin<sup>1,2†</sup>, Mingshan Xue<sup>1,3†</sup>, Yueting Jiang<sup>1</sup>, Libing Chen<sup>1</sup>, Jiahong Chen<sup>1</sup>, Yuhong Liao<sup>1</sup>, Jiali Lv<sup>1</sup>, Baojun Guo<sup>1</sup>, Peiyan Zheng<sup>1</sup>, Huimin Huang<sup>1</sup> and Baoqing Sun<sup>1,3\*</sup> 

## Abstract

**Background** The rapid emergence and global dissemination of the Omicron variant of SARS-CoV-2 have posed formidable challenges in public health. This scenario underscores the urgent need for an enhanced understanding of Omicron's pathophysiological mechanisms to guide clinical management and shape public health strategies. Our study is aimed at deciphering the intricate molecular mechanisms underlying Omicron infections, particularly focusing on the identification of specific biomarkers.

**Methods** This investigation employed a robust and systematic approach, initially encompassing 15 Omicron-infected patients and an equal number of healthy controls, followed by a validation cohort of 20 individuals per group. The study's methodological framework included a comprehensive multi-omics analysis that integrated proteomics and metabolomics, augmented by extensive bioinformatics. Proteomic exploration was conducted via an advanced Ultra-High-Performance Liquid Chromatography (UHPLC) system linked with mass spectrometry. Concurrently, metabolomic profiling was executed using an Ultra-Performance Liquid Chromatography (UPLC) system. The bioinformatics component, fundamental to this research, entailed an exhaustive analysis of protein–protein interactions, pathway enrichment, and metabolic network dynamics, utilizing state-of-the-art tools such as the STRING database and Cytoscape software, ensuring a holistic interpretation of the data.

**Results** Our proteomic inquiry identified eight notably dysregulated proteins (THBS1, ACTN1, ACTC1, POTEF, ACTB, TPM4, VCL, ICAM1) in individuals infected with the Omicron variant. These proteins play critical roles in essential physiological processes, especially within the coagulation cascade and hemostatic mechanisms, suggesting their significant involvement in the pathogenesis of Omicron infection. Complementing these proteomic insights, metabolomic analysis discerned 146 differentially expressed metabolites, intricately associated with pivotal metabolic pathways such as tryptophan metabolism, retinol metabolism, and steroid hormone biosynthesis. This comprehensive metabolic profiling sheds light on the systemic implications of Omicron infection, underscoring profound alterations in metabolic equilibrium.

**Conclusions** This study substantially enriches our comprehension of the physiological ramifications induced by the Omicron variant, with a particular emphasis on the pivotal roles of coagulation and platelet pathways

<sup>†</sup>Qianyue Yang, Zhiwei Lin, and Mingshan Xue have contributed equally to this work.

\*Correspondence:

Baoqing Sun

sunbaoqing@vip.163.com

Full list of author information is available at the end of the article



in disease pathogenesis. The discovery of these specific biomarkers illuminates their potential as critical targets for diagnostic and therapeutic strategies, providing invaluable insights for the development of tailored treatments and enhancing patient care in the dynamic context of the ongoing pandemic.

**Keywords** Omicron variant, SARS-CoV-2, Bioinformatics, Coagulation, Hemostasis

## Introduction

In November 2021, amidst the ongoing global pandemic of the novel coronavirus (SARS-CoV-2), South African scientists identified a new variant of concern (VOC), Omicron, which was promptly classified as such by the World Health Organization (WHO) on November 26, 2021 [1]. Despite increasing vaccination rates, Omicron and its subvariants continue to spread rapidly worldwide [2]. Compared to the early wild-type virus, Omicron exhibits a higher transmissibility and immune evasion capability, posing a significant public health challenge [3]. Studies have shown that both Omicron and the Delta variant can evade host immune responses through single-point mutations on the spike protein [4], with Omicron having a stronger binding affinity to receptors, thus enhancing its potential for immune evasion [5]. Although Omicron may be less pathogenic, it still poses a lethal threat to immunocompromised individuals or patients undergoing immunosuppressive therapy. The pathogenesis of Omicron is increasingly evidenced to be closely associated with cytokine storms [6], systemic inflammatory responses [6], and platelet count abnormalities [7]. The mechanisms related to platelet counts remain inadequately explained in the context of SARS-CoV-2 infection.

Platelets (PLT), key cellular components in maintaining vascular integrity and initiating hemostasis, are produced by megakaryocytes in the bone marrow and circulate in the blood as cell fragments [8]. They play a crucial role in the development, progression, and ultimate outcome of many diseases, intimately associated with platelet-mediated hemostasis and thrombosis, which may trigger adverse inflammatory responses [9]. Platelets can release serotonin and participate in immune responses by promoting T-cell activation, thus modulating immune reactions [10]. Their inherent adhesiveness allows them to interact with a variety of cells from both the innate and adaptive immune systems [11]. Studies, including that by Sevilya et al., have shown a direct link between platelet activation and SARS-CoV-2 infection [12], and it has been suggested that the expression of the angiotensin-converting enzyme 2 (ACE2) receptor and the transmembrane serine protease transmembrane serine protease 2 (TMPRSS2) on platelets and megakaryocytes play a role in mediating viral infection [13, 14]. Moreover, the functional heterogeneity of platelet aggregation is thought to

play a role in the pathogenesis of Omicron infection, contributing to the regulation of immune function within the hematological ecosystem [15].

While current research on COVID-19 pathogenesis and the coagulation/hemostasis pathways are ongoing, most studies still focus on the perspective of biomarkers [16, 17], and there are few studies on Omicron patients. This study aims to delve into the molecular interactions among key differential proteins of the Omicron variant, to identify potential targets for intervention, and to further analyze the metabolomic characteristics in the peripheral blood of Omicron patients. The urgency of this research stems from the necessity to understand the intricate interplay between the virus's pathogenesis and the host's immune response. Given the global impact of Omicron, elucidating these mechanisms is not only of scientific interest but is imperative for the development of targeted therapies and for informing public health strategies.

## Methodology

### Biospecimen collection and clinical data acquisition

The study systematically collected biospecimens and clinical data across two distinct phases: screening and validation, ensuring a robust analytical framework. In the screening phase, 15 patients diagnosed with Omicron variant infections via nucleic acid testing were recruited from the First Affiliated Hospital of Guangzhou Medical University. Diagnoses were established according to the latest COVID-19 Omicron diagnostic and treatment guidelines released by the World Health Organization, coupled with clinical symptoms and pharyngeal swab nucleic acid test results. Additionally, 15 healthy volunteers, matched by age and gender, were selected as controls. Comprehensive demographic, clinical, and laboratory data were compiled for both groups, followed by serum collection for in-depth proteomic and metabolomic analyses. The validation phase further substantiated our initial findings through an expanded cohort of 20 Omicron patients and 20 controls, employing identical proteomics methodologies and Receiver operating characteristic (ROC) analyses to ensure the reproducibility and validity of our screening phase outcomes. Informed consent was obtained from all participants, and the study protocol was approved by the Ethics Committee of the First Affiliated Hospital of Guangzhou Medical

University (Ethical Approval Numbers: 202001134 and 202115202). A schematic representation of the study design can be found in Fig. 1.

**Proteomic analysis**

Upon thawing, serum samples were treated with methanol/acetonitrile (1:1, volume ratio, Sigma-Aldrich, St. Louis, MO, USA) to achieve a total volume ratio of 2:2:1 (excluding water). The samples were vortexed on ice for 30 s, subjected to high-intensity ultrasonication for 10 min, and then left to stand at -20 °C for one hour. Subsequently, the samples were centrifuged at 4 °C (12,000g, 15 min), and the supernatant was collected and dried at room temperature. The dried samples were reconstituted in acetonitrile/water (1:1, volume ratio, Sigma-Aldrich, St. Louis, MO, USA), vortexed and ultrasonicated again, and centrifuged to remove any precipitate. The supernatant was stored at -80 °C until analysis. The samples were resolved in solvent A (0.1% formic acid in 2% acetonitrile/water, Sigma-Aldrich, St. Louis, MO, USA) and

separated using a homemade reverse-phase liquid chromatography column (25 cm length, 75/100 μm inner diameter). Chromatographic separation was carried out on a nanoElute Ultra-High-Performance Liquid Chromatography (UHPLC) system (Bruker Daltonics, Billerica, MA, USA) at a flow rate of 450 nL/min, followed by electrospray ionization through a capillary source and mass spectrometric analysis using a timsTOF Pro (Bruker Daltonics, Billerica, MA, USA) in PASEF mode with a dynamic exclusion time of 30 s.

**Metabolomic analysis**

Metabolite separation was conducted using a Waters ACQUITY UltraPerformance Liquid Chromatography (Waters ACQUITY UPLC) System (Waters Corporation, Milford, MA, USA) equipped with a BEH C18 column. Chromatographic conditions included a 10 μL injection volume, a flow rate of 400 μL/min, and a column temperature maintained at 40 °C. Metabolomics data were processed using MassLynx (Waters Corporation, Milford,

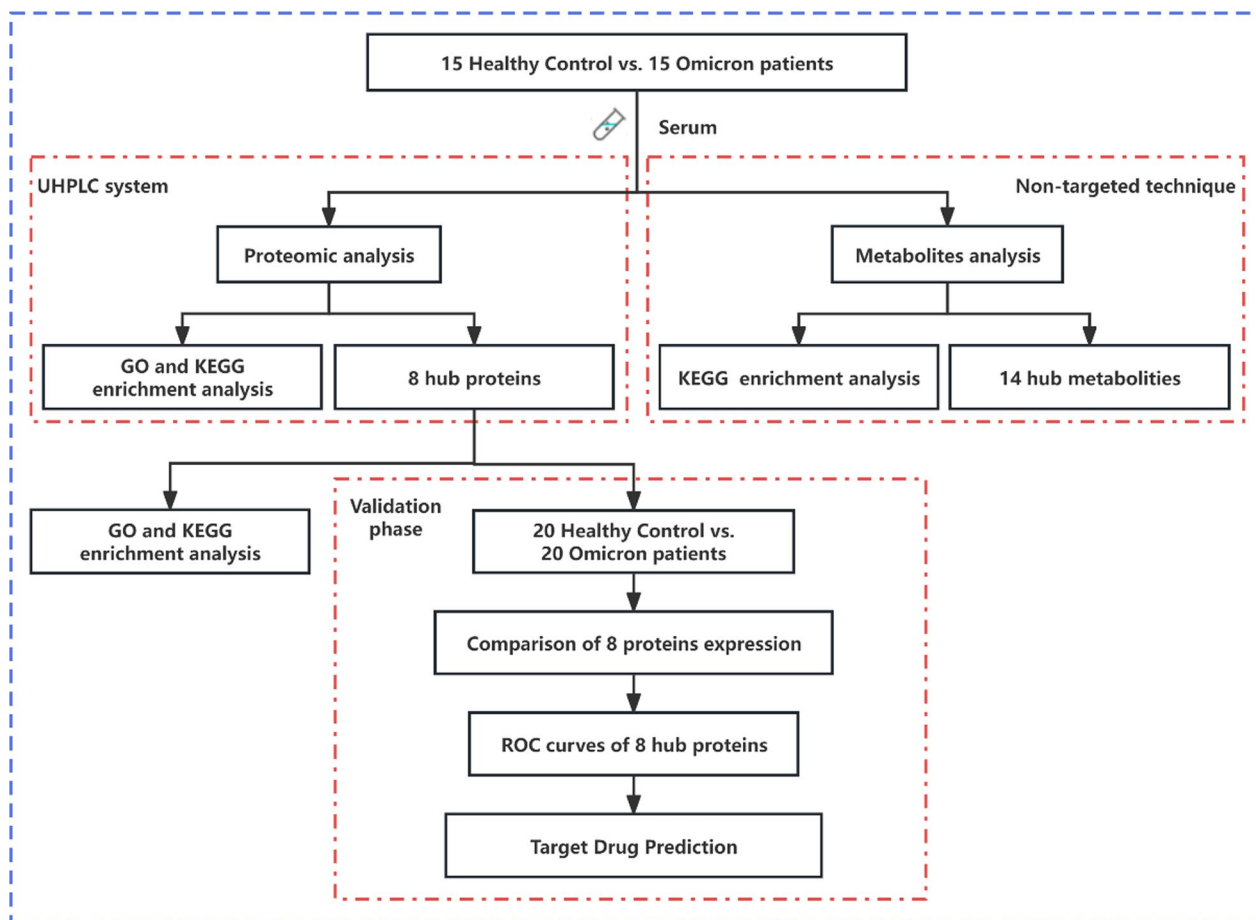


**Fig. 1** A visual representation of the study design. It is mainly divided into three parts: proteomics detection, metabolomics detection and validation queue detection. This structured approach ensures a thorough analysis of the biological samples, integrating proteomic and metabolomic data to validate the identified biomarkers and pathways relevant to the study's focus

MA, USA), which entailed peak extraction, alignment, and retention time correction, ensuring that the mass accuracy was controlled within 20 ppm to guarantee data accuracy.

**Bioinformatics analysis**

Proteomics data were analyzed using the limma package in R software (version 3.6.3) to identify differentially expressed proteins (DEPs) with  $p < 0.05$  and  $\text{Log}_2\text{FC} > 1$  [18, 19]. Heatmaps, volcano plots, and boxplots were generated using the "heatmap" and "ggplot2" packages in R (version 3.3.3). Proteins were annotated using the UniProt-GOA database (<http://www.ebi.ac.uk/GOA>), and enriched pathways were determined using Kyoto Encyclopedia of Genes and Genomes (KEGG) analysis. Protein–protein interaction networks (PPI) for the DEPs were constructed using the STRING database (<https://string-db.org/>), and further analysis of the PPI was carried out in Cytoscape software using cytohubba and MCODE plugins to identify and analyze key hub proteins, which were then subjected to GO/KEGG enrichment analysis.

Metabolomics data were normalized and integrated using support vector regression and analyzed for significant differences using orthogonal partial least squares-discriminant analysis (OPLS-DA). Variable importance in projection (VIP) values were calculated for each metabolite, with a  $\text{VIP} > 1$  considered significant ( $P < 0.05$ ) [20]. Pathway enrichment analysis for these differentially expressed metabolites was performed using GO/KEGG databases to identify significantly enriched pathways.

**Prediction of potential therapeutic agents**

The DSigDB database (<http://tanlab.ucdenver.edu/DSigDB>) was utilized to predict potential therapeutic agents for COVID-19 based on protein–drug interaction data. The thresholds set for selection were False Discovery Rate (FDR)  $< 0.05$  and composite score  $> 5000$ .

**Statistical analysis**

Statistical analyses were conducted using SPSS software version 27.0, with continuous variables expressed as median and interquartile range (IQR). The Mann–Whitney U test (for two groups) and independent samples t-test were employed to assess differences in continuous variables. A  $P < 0.05$  was considered statistically significant. Receiver operating characteristic (ROC) curves were plotted using Graphpad Prism software (version 9.5.1) to determine the sensitivity and specificity of hub genes. The area under the ROC curve (AUC) was measured, with an  $\text{AUC} > 0.7000$  indicating diagnostic significance for the differentially expressed proteins.

**Results**

**Clinical characteristics of the screening cohort**

In terms of clinical parameters, compared to the healthy control group, the Omicron patient group exhibited elevated levels of Neutrophil percentage (NEU%), Monocyte count and percentage (MONO% and MONO), Basophils percentage (BASO%), International Normalized Ratio (INR), Fibrinogen (FIB), D-Dimer (D-D), C-reactive protein (CRP), Serum Amyloid A (SAA), and Procalcitonin (PCT) ( $P < 0.05$ ). Conversely, there was a significant decrease in Lymphocyte count and percentage (LYM% and LYM), Eosinophils count and percentage (EOS and EOS%), Basophil count (BASO), and Prothrombin Time Activity (PTTA) ( $P < 0.05$ ). These differences were statistically significant (Table 1).

**Proteomic profile and functional alterations associated with omicron**

Using the UHPLC system, a total of 746 proteins were identified in the serum samples of both groups. Based

**Table 1** Basic information of healthy controls and omicron patients

	Healthy controls	Omicron	P
N	15	15	
Age	49.00 (37.00–61.00)	45.00 (29.00–57.00)	0.578
WBC, $10^9/\text{L}$	5.90 (4.80–6.60)	5.33 (4.12–7.17)	0.817
NEU %	58.20 (52.20–62.30)	67.90 (59.20–76.20)	0.024
LYM %	29.80 (27.80–37.60)	18.80 (13.00–30.10)	0.002
MONO %	6.60 (6.40–8.20)	10.10 (8.50–13.70)	0.001
EOS %	3.20 (1.50–4.00)	0.40 (0.30–1.10)	$< 0.001$
BASO %	0.13 (0.12–0.23)	0.42 (0.41–0.66)	$< 0.001$
NEU, $10^9/\text{L}$	3.40 (3.00–3.70)	3.71 (2.59–5.03)	0.380
LYM, $10^9/\text{L}$	1.80 (1.60–2.20)	1.30 (0.69–1.39)	$< 0.001$
MONO, $10^9/\text{L}$	0.42 (0.40–0.51)	0.57 (0.42–0.87)	0.040
EOS, $10^9/\text{L}$	0.19 (0.16–0.22)	0.02 (0.01–0.06)	$< 0.001$
BASO, $10^9/\text{L}$	0.07 (0.05–0.08)	0.03 (0.02–0.04)	$< 0.001$
PT, S	12.80 (12.50–13.50)	12.80 (11.30–15.30)	0.844
INR	0.60 (0.40–0.90)	0.98 (0.85–1.35)	$< 0.001$
PTTA, %	96.00 (87.00–106.00)	82.00 (73.00–89.00)	0.004
FIB, g/L	3.22 (2.45–3.26)	3.48 (3.31–3.65)	0.003
APTT, S	33.10 (32.10–36.20)	36.40 (32.20–41.20)	0.171
TT, S	16.20 (15.50–17.80)	17.80 (16.20–18.20)	0.224
D-Dimer, $\mu\text{g}/\text{L}$	333.00 (258.00–364.00)	486.00 (452.00–852.00)	$< 0.001$
CRP, mg/dL	2.50 (1.70–3.00)	5.30 (2.82–9.44)	0.005
SAA, mg/L	6.30 (2.90–8.40)	43.60 (29.40–67.60)	$< 0.001$
PCT, ng/mL	0.02 (0.01–0.04)	0.09 (0.05–0.14)	$< 0.001$

WBC White blood cell, NEU Neutrophil, LYM Lymphocyte, MONO Monocyte, EOS Eosinophils, BASO Basophil, PT Prothrombin time, INR International normalized ratio, PTTA Prothrombin activity, FIB Fibrinogen, APTT Activated partial thromboplastin time, TT Thrombin, DD D-Dimer, CRP C-reactive protein, SAA Serum amyloid A, PCT Procalcitonin



on the criteria of  $|\log_2(\text{FC})| > 1$  and  $p\text{-value} < 0.05$ , a total of 27 differentially expressed proteins (DEPs) were identified, which included 15 upregulated proteins and 12 downregulated proteins, as shown in Fig. 2A (Additional file 1: Table S1). Principal Component Analysis (PCA), conducted using the normalized expression matrix, confirmed the variability between the proteomes of the samples (Fig. 2B). The heatmap of the aforementioned differentially expressed proteins is depicted in Fig. 2C.

GO and KEGG enrichment analyses were conducted on the differentially expressed proteins (Additional file 1: Table S2). These proteins were significantly enriched in GO pathways related to hemostasis, coagulation, and blood clotting, and were significantly enriched in the KEGG pathways related to Shigella and focal adhesion kinase pathways (Figs. 2D–H).

### Selection and functional enrichment analysis of omicron hub proteins

Protein–protein interaction networks were constructed using the STRING database (Fig. 3A), and core hub proteins for both groups were identified through the MCC algorithm of the cytohubba plugin in Cytoscape software (Fig. 3C), leading to the selection of 10 hub proteins: THBS1, ACTN1, ACTC1, POTEF, ACTB, TPM4, VCL, ICAM1, PARK7, and YWHAB. Further analysis confirmed 8 of these hub proteins by MCODE: THBS1, ACTN1, ACTC1, POTEF, ACTB, TPM4, VCL, and ICAM1 (Fig. 3B). Venn diagrams from both methods confirmed the 8 common differentially expressed hub proteins (Fig. 3D). Heatmap analysis revealed an upregulated trend in Omicron patients compared to the healthy control group for all hub proteins except THBS1 (Fig. 3E).

Enrichment analysis of the 8 differentially expressed hub proteins was performed using GO/KEGG pathways (Additional file 1: Table S3). The results showed that the most enriched GO pathways included hemostasis, coagulation, and platelet aggregation, while the most enriched KEGG pathways were focal adhesion kinase, leukocyte transendothelial migration, Shigella, and actin cytoskeleton among others (Figs. 3F, G).

### Clinical characteristics of the validation cohort

In the validation cohort, significant differences were observed when comparing Omicron patients ( $n=20$ ) to the healthy control group ( $n=20$ ). There was a notable increase in Neutrophil percentage (NEU%), Monocyte percentage (MONO%), Prothrombin time (PT), Fibrinogen (FIB), Activated partial thromboplastin time (APTT), D-Dimer (D-D), C-reactive protein (CRP), Serum amyloid (SAA), and Procalcitonin (PCT) levels ( $P < 0.05$ ) in the Omicron patients. Conversely, a significant decrease was found in Lymphocyte percentage (LYM% and LYM), Eosinophils (EOS), Basophil percentage (BASO%), and Prothrombin Activity (PTTA) ( $P < 0.05$ ). These differences were statistically significant (Table 2).

### Validation of differential hub protein expression and diagnostic value

The validation phase confirmed that the eight differentially expressed hub proteins significantly differed between the healthy control group and Omicron patients ( $P < 0.05$ ) (Fig. 4A–H), also demonstrating diagnostic significance (Fig. 4I–P). Specifically, the area under the curve (AUC) for THBS1 was 0.7125 (95% CI 0.5527–0.8723), for ACTN1 it was 0.8450 (95% CI 0.7247–0.9653), for ACTC1 it was 0.8025 (95% CI 0.6672–0.9378), for POTEF 0.8025 (95% CI 0.6667–0.9383), for ACTB 0.7300 (95% CI 0.5733–0.8867), for TPM4 0.8250 (95% CI 0.6924–0.9576), for VCL 0.8775 (95% CI 0.7743–0.9807), and for ICAM1 0.7605 (95% CI 0.6113–0.9187).

### Omicron-associated metabolomic features and functional changes

Through the application of 4D non-targeted metabolomics techniques, we identified 146 differentially expressed metabolites (DEMs) out of 357 metabolites (Additional file 1: Table S4). Quality control was performed based on the distribution of the total metabolites by group. Orthogonal partial least squares-discriminant analysis (OPLS-DA) demonstrated a clear separation between the healthy control group and the Omicron group, indicating distinctive metabolomic profiles (Fig. 5A). A volcano plot revealed the expression differences among all metabolites, with 27 being upregulated and 57 downregulated

(See figure on next page.)

**Fig. 2** Analysis procedures for subject inclusion and overall analysis of bioinformation. **A** The volcano plots of differentially expressed proteins (DEPs); **B** Principal Component Analysis (PCA) of 2 Groups; **C** Heatmap of DEPs; **D, E** Gene Ontology (GO) and Kyoto Encyclopedia of Genes and Genomes (KEGG) analyses reveal the functional categories and pathways enriched among the 27 DEPs. The GO analysis primarily focuses on hemostasis, platelet alpha granule, and integrin binding pathways. The KEGG analysis emphasizes pathways associated with shigellosis, focal adhesion, and leukocyte transendothelial migration. **F–H** Chord diagrams illustrate the intricate relationships between GO/KEGG terms. *BP* Biological process, *CC* Cellular component, *MF* Molecular function, *PCA* principal component analysis

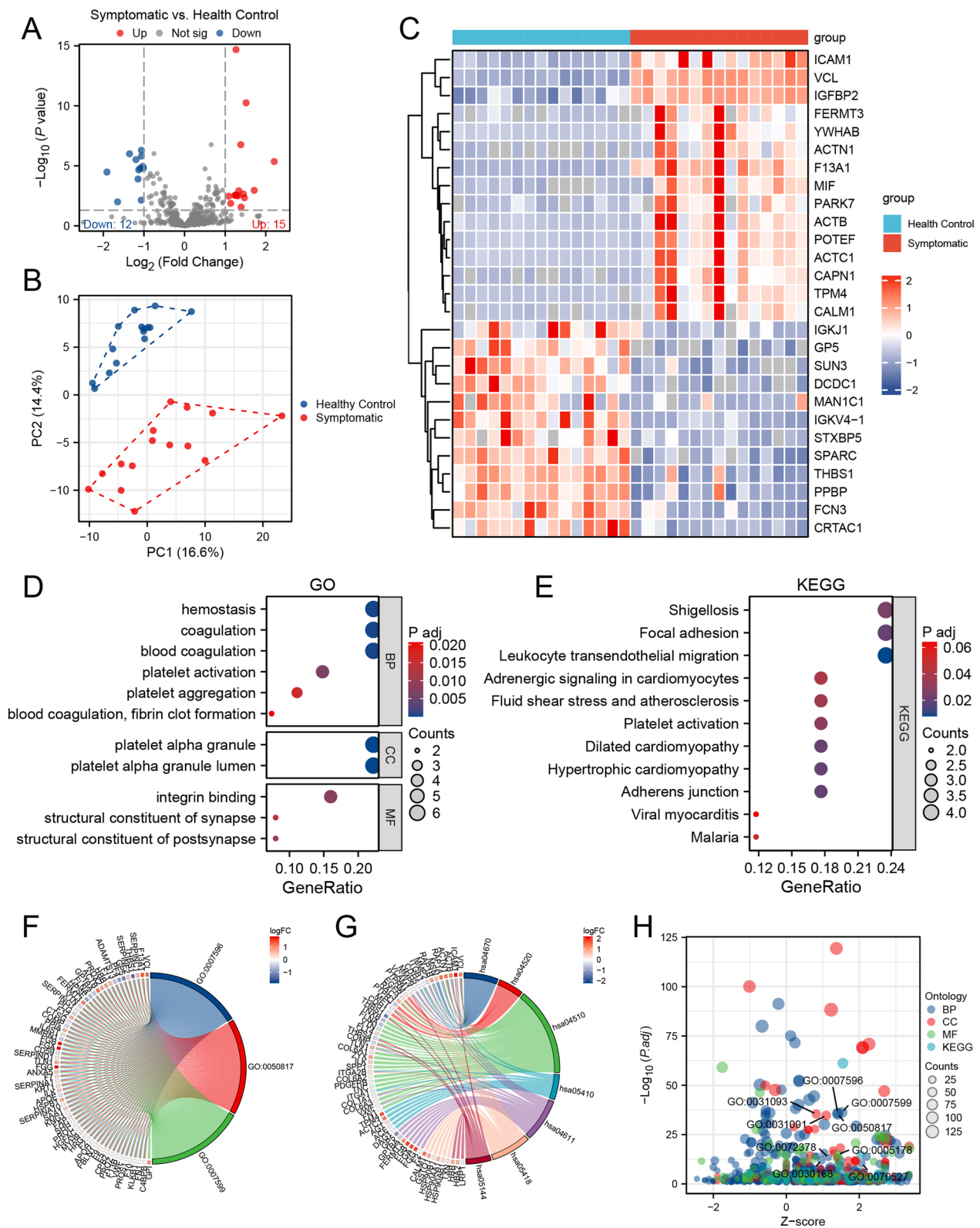


**Fig. 2** (See legend on previous page.)

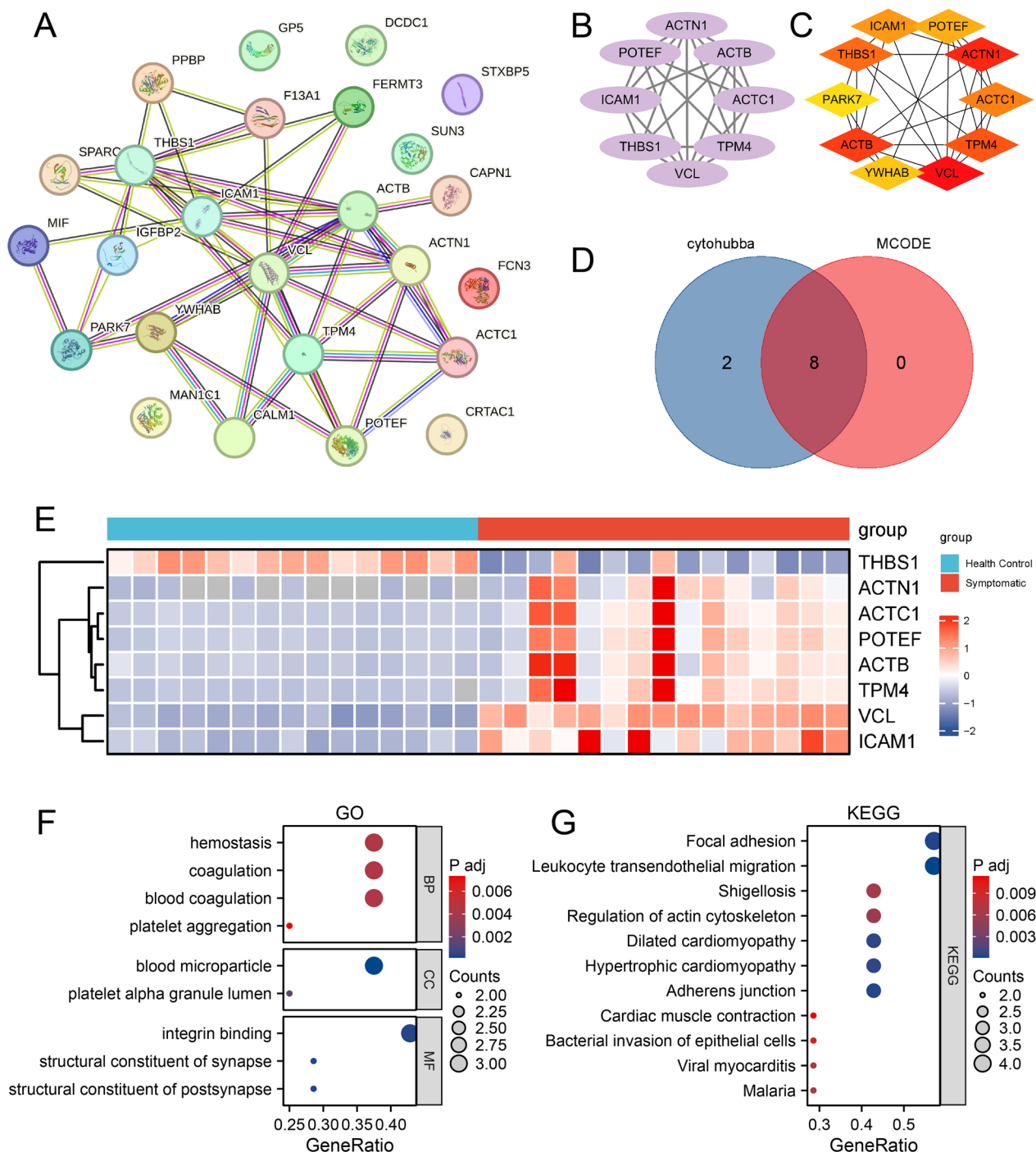


**Fig. 3** Secondary screening of functional pathway core protein sites. **A** STRING of 27 differentially expressed proteins (DEPs); **B** 8 MCODE hub genes: THBS1, ACTN1, ACTC1, POTEF, ACTB, TPM4, VCL, and ICAM1; **C** 10 cytohubba-MCC hub genes: THBS1, ACTN1, ACTC1, POTEF, ACTB, TPM4, VCL, ICAM1, PARK7, and YWHAB; **D** Venn of MCODE hub genes and cytohubba-MCC hub genes: THBS1, ACTN1, ACTC1, POTEF, ACTB, TPM4, VCL, and ICAM1; **E** Heatmap of 8 hub proteins. **F, H** Gene Ontology (GO) analysis reveals enrichment in hemostasis, blood microparticle, and integrin binding pathways, while Kyoto Encyclopedia of Genes and Genomes (KEGG) pathways focus on focal adhesion, leukocyte transendothelial migration, and shigellosis

**Table 2** Basic information of participants in the second batch verification queue

	Healthy controls	Omicron	P
N	20	20	
Age	54.00 (36.75–58.75)	53.00 (46.00–62.00)	0.580
WBC, 10 <sup>9</sup> /L	6.64 (5.35–9.27)	5.80 (4.62–7.85)	0.229
NEU %	53.88 (44.30–61.44)	92.66 (73.34–105.28)	<0.001
LYM %	29.37 (26.30–34.81)	16.71 (13.34–28.89)	<0.001
MONO %	6.98 (5.34–8.29)	12.33 (10.61–14.60)	<0.001
EOS %	1.45 (0.88–3.38)	1.65 (0.93–2.10)	0.839
BASO %	0.86 (0.38–1.13)	0.17 (0.10–0.22)	<0.001
NEU, 10 <sup>9</sup> /L	5.00 (3.67–6.05)	5.28 (2.65–5.53)	0.655
LYM, 10 <sup>9</sup> /L	2.40 (1.80–3.15)	1.50 (0.80–2.30)	0.004
MONO, 10 <sup>9</sup> /L	0.44 (0.26–0.65)	0.42 (0.37–0.66)	0.960
EOS, 10 <sup>9</sup> /L	0.22 (0.16–0.37)	0.15 (0.08–0.21)	0.004
BASO, 10 <sup>9</sup> /L	0.02 (0.01–0.03)	0.03 (0.02–0.03)	0.194
PT, S	12.45 (11.73–13.40)	14.00 (12.85–14.58)	0.003
INR	0.75 (0.60–0.90)	0.90 (0.80–1.18)	0.060
PTTA, %	97.00 (92.43–109.00)	83.20 (76.25–94.10)	<0.001
FIB, g/L	2.90 (2.53–3.45)	4.74 (3.53–5.52)	<0.001
APTT, S	35.70 (31.50–40.15)	41.40 (31.85–47.18)	0.048
TT, S	16.15 (15.23–18.78)	16.55 (15.20–18.33)	0.745
D-Dimer, µg/L	297.00 (211.00–364.75)	510.00 (439.50–603.50)	<0.001
CRP, mg/dL	2.75 (1.65–4.13)	8.50 (5.80–10.40)	<0.001
SAA, mg/L	5.50 (3.10–8.38)	35.75 (30.48–44.88)	<0.001
PCT, ng/mL	0.02 (0.01–0.05)	0.09 (0.06–0.15)	<0.001

WBC White blood cell, NEU Neutrophil, LYM Lymphocyte, MONO Monocyte, EOS Eosinophils, BASO Basophil, PT Prothrombin time, INR International normalized ratio, PTTA Prothrombin activity, FIB Fibrinogen, APTT Activated partial thromboplastin time, TT Thrombin, DD D-Dimer, CRP C-reactive protein, SAA Serumamyloid A, PCT Procalcitonin

(Fig. 5B). A heatmap displayed the top 50 differential metabolites between the two groups, underscoring the metabolic disparities (Fig. 5C). These differentially expressed metabolites were primarily enriched in pathways related to tryptophan metabolism, retinol metabolism, and steroid hormone biosynthesis, among others (Fig. 5D, E).

**Target drug prediction**

The DSigDB database was used to predict potential target drugs associated with eight differentially expressed hub proteins that may treat Omicron infection by modulating the hub proteins. A total of 714 target drugs were finally predicted; the composite scores and corresponding target genes are listed in Additional file 1: Table S5. The top 10 predicted target drugs according to the composite scores are shown in Fig. 6.

**Discussion**

Amid the current global health crisis, the rapid transmission of the Omicron variant has had profound impacts on economies and public health systems worldwide. Omicron, with its enhanced ability to evade the immune system, has shown significant transmissibility compared to previous SARS-CoV-2 strains [21]. Although our understanding of the host response dynamics to this new variant is limited, identifying biomarkers that can predict disease progression or assist in diagnosis is vital to meet the challenges posed by Omicron. Our study integrates clinical diagnostics with multi-omics analyses to compare biomarkers between individuals infected with Omicron and healthy subjects, identifying eight differentially expressed hub proteins—THBS1, ACTN1, ACTC1, POTEE, ACTB, TPM4, VCL, and ICAM1.

Significant mutations in the spike protein of Omicron enhance its ability to evade immune responses [22], which may be associated with severe clinical outcomes such as cerebral embolism, deep vein thrombosis, and respiratory failure [23]. These findings resonate with studies positioning antithrombin as a broad-spectrum inhibitor of coronavirus infection, suggesting that the coagulation pathway may be a key element in the course of Omicron infection [24]. However, the specific relationship between Omicron and the coagulation pathway has not yet been elucidated. Therefore, the relationship between the coagulation pathway and Omicron warrants deeper investigation. This study’s analysis of coagulation markers, including Activated Partial Thromboplastin Time (APTT), Fibrinogen (FIB), and D-Dimer, in patients infected with the Omicron variant reveals significant alterations when compared to healthy individuals. These changes underscore a pronounced association with hemostasis, coagulation, and blood clotting pathways, mirroring the conclusions drawn in earlier research [25]. Further substantiating these findings, our GO and KEGG pathway analyses on eight central hub proteins identified a pronounced enrichment in biological pathways directly tied to hemostasis, coagulation, and blood clotting. This enrichment not only corroborates the observed changes in coagulation markers but also suggests that Omicron infection might precipitate distinct alterations in the biological processes integral to these pathways.

The interplay between inflammation and coagulation is well recognized, with inflammation able to trigger coagulation mechanisms, and vice versa [26]. In the context of COVID-19, the activation of coagulation and hemostasis pathways is considered to be mediated by the inflammatory system’s tissue factors [27]. Even though Omicron exhibits biological characteristics different from previous variants, severe infections may still induce platelet activation and partial desensitization, thereby affecting the



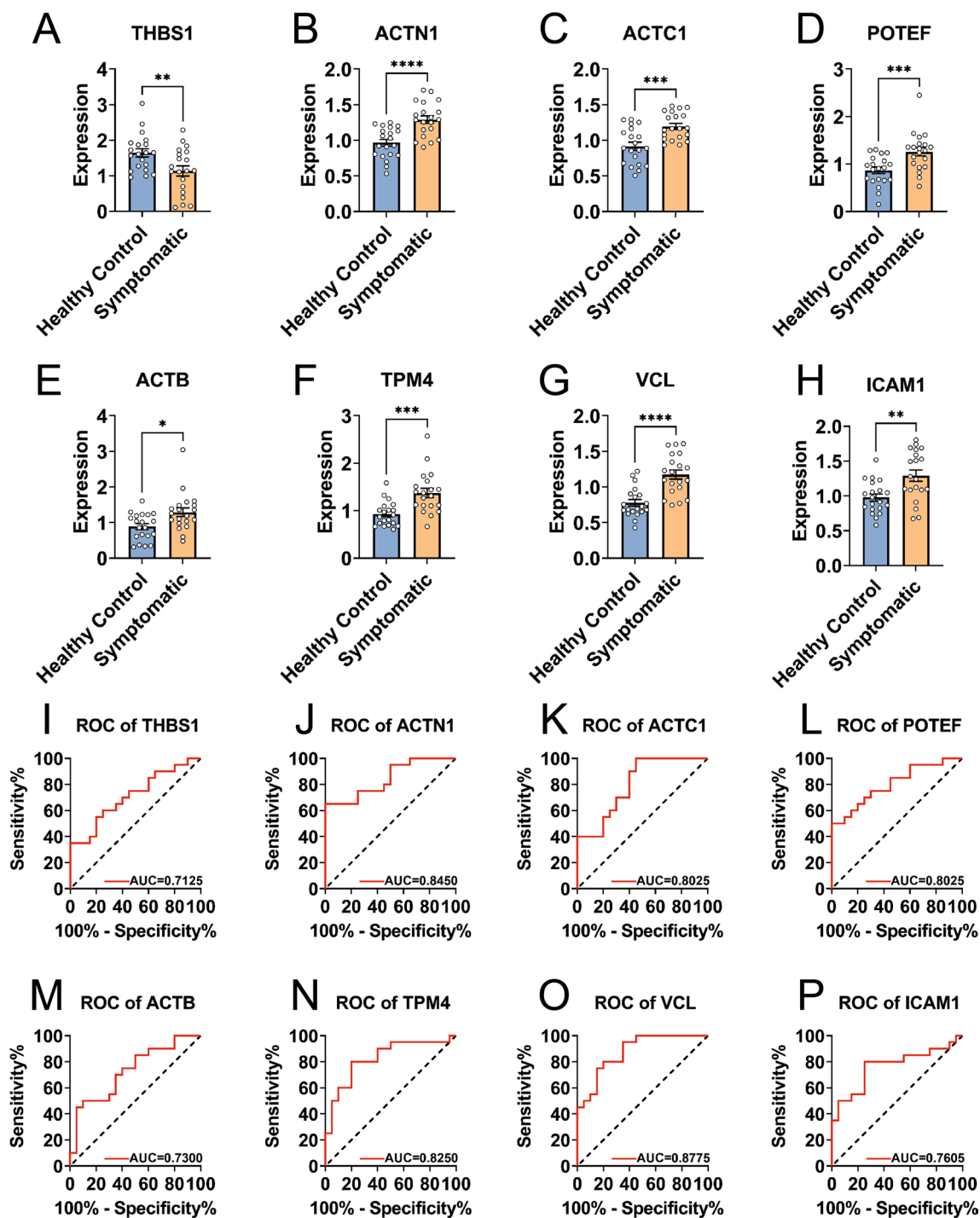


**Fig. 4** Validation of core protein expression in the validation cohort. **A–H** This series compares the expression levels of eight key proteins between Omicron-infected and healthy individuals, illustrating significant differences. **I–P** Diagnostic Receiver Operating Characteristic (ROC) curves for the same eight core proteins demonstrate their potential as biomarkers for distinguishing between Omicron and healthy samples. The Area Under the Curve (AUC) for all eight hub proteins exceeds 0.7, indicating a promising diagnostic capability. \* $P < 0.05$ . \*\* $P < 0.01$ . \*\*\* $P < 0.001$ . ROC receiver operating characteristic, AUC Area under Curve

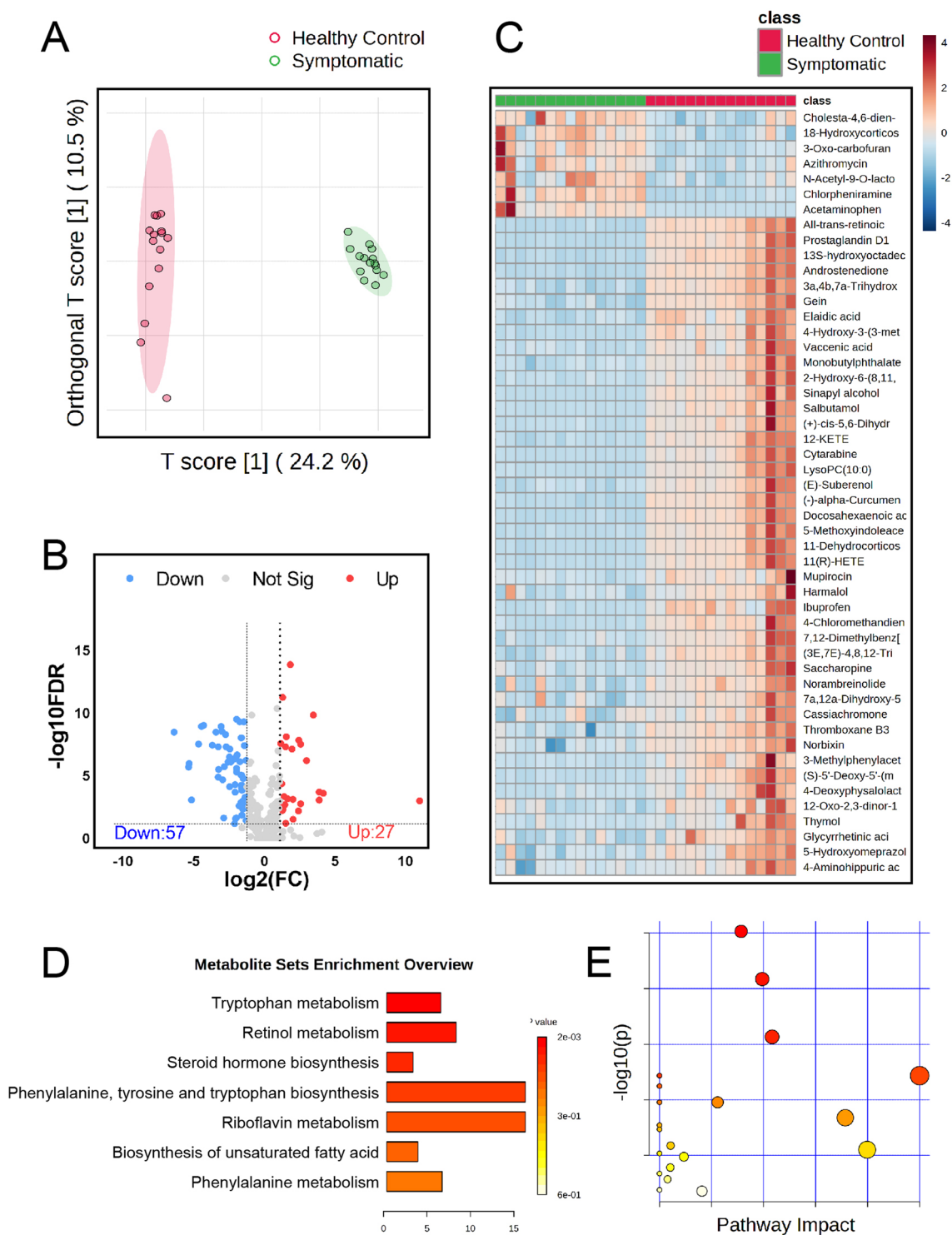
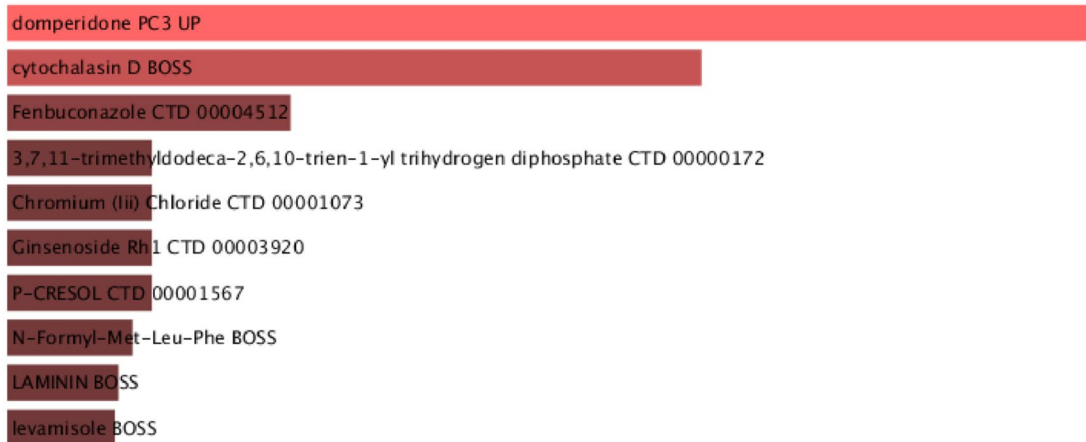


**Fig. 5** Metabolomics analysis. **A** Orthogonal Partial Least Squares-Discriminant Analysis (OPLS-DA) differentiates between healthy controls and Omicron-infected groups; **B** Volcano plots reveal Differentially Expressed Metabolites (DEMs) between the two groups; **C** A heatmap illustrates the expression patterns of DEMs, highlighting significant variations; **D, E** Gene Ontology (GO) and Kyoto Encyclopedia of Genes and Genomes (KEGG) analyses show that the identified metabolites are predominantly enriched in tryptophan metabolism, retinal metabolism, and steroid hormone biosynthesis pathways

**A**



**B**

Index	Name	P-value	Adjusted p-value	Odds Ratio	Combined score
1	domperidone PC3 UP	0.00002650	0.004461	369.89	3897.96
2	cytochalasin D BOSS	0.00004181	0.004461	289.41	2917.92
3	Fenbuconazole CTD 00004512	0.00008275	0.006556	201.61	1895.03
4	3,7,11-trimethyldodeca-2,6,10-trien-1-yl trihydrogen diphosphate CTD 00000172	0.004392	0.03641	285.46	1549.44
5	Chromium (Iii) Chloride CTD 00001073	0.004392	0.03641	285.46	1549.44
6	Ginsenoside Rh1 CTD 00003920	0.004392	0.03641	285.46	1549.44
7	P-CRESOL CTD 00001567	0.004392	0.03641	285.46	1549.44
8	N-Formyl-Met-Leu-Phe BOSS	0.0001196	0.008074	166.27	1501.64
9	LAMININ BOSS	6.197e-7	0.0004418	102.59	1466.36
10	levamisole BOSS	0.0001254	0.008074	162.20	1457.25

**Fig. 6** Top 10 Predicted Target Drugs. The top 10 predicted target drugs for combating Omicron infection, based on composite scores from DSigDB, are showcased. **A** Highlights the predicted target drugs that modulate the hub genes, with a bar graph illustrating their potential effectiveness. Notably, Domperidone and Cytochalasin D emerge as promising candidates for treating Omicron infection by targeting these eight critical proteins. **B** A table in DSigDB provides a detailed overview of these drugs and their associated scores, underlining their potential therapeutic value

coagulation pathway [28], and the coagulation pathway plays a significant role in regulating pulmonary fibrosis, hemostatic disorders, and surfactant damage [29]. VCL, a protein located at the cytoplasmic face of cellular matrix and intercellular adhesions, is involved in linking integrins to the F-actin cytoskeleton and can act as a mechanical sensor transmitting forces to maintain cellular shape, serving as a dynamic regulator of cell adhesion [30, 31]. The high expression of VCL can enhance cellular adhesiveness, and its regulatory role in adhesion is crucial for biological processes such as leukocyte transmigration through epithelial or endothelial layers, thereby mediating the migration of leukocytes in the inflammatory response of COVID-19 [32]. ACTB protein, also known as  $\beta$ -actin, plays a vital role in various cellular processes

such as cell division, migration, invasion, vesicle transport, and cellular structural regulation[33]. ACTB can modulate endothelial nitric oxide synthase activity, altering NO production and thus causing endothelial dysfunction, activating coagulation pathways and inflammatory responses [34]. THBS1 is a matrix glycoprotein released by activated platelets, involved in angiogenesis, inflammatory responses, platelet aggregation, cell apoptosis, and fibrosis [35]. A decline in THBS1 expression is associated with oxidative stress damage [36], and THBS1 is involved in the fibrin clot response to injury [37]. Furthermore, silencing of THBS1 can inhibit the activation of the NLRP3 inflammasome, reducing the levels of inflammatory cytokines, thereby reducing pneumonia caused by cytokine storms [38]. POTEF, as a member of

the POTE ankyrin domain family, can regulate TLR signaling which is critical in innate immunity and is expressed in immune cells playing a significant role during cell invasion [39], and it can inhibit apoptosis and promote cell growth [40]. However, the role of POTE in pneumonia caused by Omicron is not clear, and our findings suggest that POTE is involved in tissue coagulation processes, participating in disease inflammation and cell regulatory responses.

ACTN1 is a cytoskeletal actin-binding protein [41] that, in addition to mediating sarcomere function, performs important non-muscle functions, such as the regulation of cytokinesis, cell adhesion, and migration [42]. Our study found that high expression of ACTN1 is associated with cell adhesion and is a significant factor in the development and progression of Omicron. ACTC1 is a cardiac-related protein expressed in regenerating muscle fibers in diseased mature skeletal muscle [43], and our study shows that in the Omicron group, ACTC1 expression is elevated through the actin filament organization pathway. TPM4 is a key actin-binding protein [44], and studies have shown that TPM4 expression is strongly increased in the later stages of megakaryocyte formation and that TPM4 has a functional role in thrombus formation in mammals [45, 46]. This is consistent with our findings, which indicate that TPM4 can act as a promoter in pathways such as focal adhesion, mediating the occurrence, development, and outcome of the disease. Studies suggest that focal adhesion is associated with mechanisms of cell migration [47], which can regulate mechanotransduction, cell migration, cell cycle progression, proliferation differentiation, growth, and repair [48], and our study finds focal adhesion to be related to the pathological process of the disease. Additionally, ICAM-1 is a cell surface glycoprotein and adhesion receptor that, besides being expressed on vascular endothelial cells, also functions on epithelial and immune cells, affecting inflammatory stimulation [49]. Studies indicate that ICAM-1 is associated with leukocyte-endothelial cell interactions and solute permeability changes [50]. Our study suggests that ICAM-1 has a significant association with the inflammatory exudation and endothelial barrier establishment caused by Omicron.

In addition, the tryptophan pathway can be affected by systemic inflammatory signaling factors, promoting immune suppression and evasion of immune surveillance in inflammation [51], thereby helping to suppress inflammation caused by Omicron. L-tryptophan is an essential amino acid that produces a variety of signal molecules through complex metabolic pathways [52, 53]. Studies also suggest that the L-tryptophan pathway can achieve immune suppression by depleting tryptophan, depriving proliferating T cells of essential amino acids [52,

53]. Indole-3-acetate (I3A), a metabolite depleted in the context of the microbiome and high-fat diets, has been proven to reduce the production of pro-inflammatory cytokines and inhibit cell migration towards chemokines, achieving the effect of alleviating inflammation [54]. These are consistent with our findings.

This study highlights the therapeutic potential of targeting eight differentially expressed proteins in treating Omicron infection, with Domperidone and Cytochalasin D being particularly noteworthy. Domperidone's antiviral properties, as demonstrated by stimulating prolactin secretion, suggest a dual role in enhancing both innate and adaptive immune responses [55], aligning with our findings and highlighting the necessity for further research on its clinical application parameters. Similarly, Cytochalasin D's inhibition of actin polymerization and its capacity to reverse PLT-induced suppression of cell apoptosis present a novel therapeutic pathway worth exploring [56].

The study acknowledges several limitations, such as the complexity of interpreting metabolomic data, which necessitates advanced bioinformatics and further biological validation. While eight potential biomarkers were identified, their clinical significance requires validation in a more diverse population. The absence of direct mechanistic evidence, focusing instead on associations, calls for further research to clarify how these changes affect disease progression. Despite these challenges, the study offers a comprehensive view of Omicron's pathophysiology, contributing valuable insights into coagulation and inflammation and underscoring the need for continued research to develop targeted clinical and public health strategies.

## Conclusion

In conclusion, our study highlights the significant impact of the Omicron variant on clinical and molecular levels. The identified hub proteins, enriched in coagulation and inflammatory pathways, underscore the intricate interplay between the inflammatory response and coagulation system in the context of Omicron infection. The biomarkers discovered offer a valuable resource for potential diagnostic and prognostic applications. While Omicron's unique biological characteristics necessitate further investigation, our findings contribute to the understanding of the pathophysiological mechanisms behind its clinical manifestations. However, the limitations of our study, include a call for further research with larger cohorts to validate these biomarkers and unravel the mechanisms of Omicron-induced pathology. Our work lays the groundwork for future studies aimed at developing targeted interventions to mitigate the effects of this challenging variant.



**Abbreviations**

SARS-CoV-2	Severe acute respiratory syndrome coronavirus 2
VOC	Variant of concern
PLT	Platelets
WHO	The World Health Organization
ACE2	Angiotensin-converting enzyme 2
TMPRSS2	Transmembrane serine protease 2
COVID-19	Corona Virus Disease 2019
UHPLC	Ultra-high-performance liquid chromatography
UPLC	Ultra-performance liquid chromatography
DEPs	Differentially expressed proteins
DEMs	Differentially expressed metabolites
Log <sub>2</sub> FC	Log <sub>2</sub> FoldChange
GO	Gene ontology
KEGG	Kyoto encyclopedia of genes and genomes
PPI	Protein–protein interaction networks
OPLS-DA	Orthogonal partial least squares-discriminant analysis
VIP	Variable importance in projection
FDR	False discovery rate
IQR	Interquartile range
ROC	Receiver operating characteristic
AUC	The area under the curve
WBC	White blood cell
NEU	Neutrophil
LYM	Lymphocyte
MONO	Monocyte
EOS	Eosinophils
BASO	Basophil
PT	Prothrombin time
INR	International normalized ratio
PTTA	Prothrombin activity
FIB	Fibrinogen
APTT	Activated partial thromboplastin time
TT	Thrombin
DD	D-Dimer
CRP	C-reactive protein
SAA	Serum amyloid A
PCT	Procalcitonin
BP	Biological process
CC	Cellular component
MF	Molecular function
PCA	Principal component analysis
95% CI	95% Confidence interval
I3A	Indole-3-acetate
THBS1	Thrombospondin 1
ACTN1	Alpha-actinin 1
ACTC1	Actin alpha cardiac muscle 1
POTEF	POTE ankyrin domain family member F
ACTB	Actin beta
TPM4	Tropomyosin 4
VCL	Vinculin
ICAM1	Intercellular adhesion molecule 1
PARK7	Parkinsonism associated deglycase
YWHAB	Tyrosine 3-Monooxygenase/Tryptophan 5-Monooxygenase Activation Protein Beta

**Supplementary Information**

The online version contains supplementary material available at <https://doi.org/10.1186/s12967-024-05022-z>.

**Additional file 1:** Table S1–Table S5.

**Acknowledgements**

We thank the Immunology Department of the First Affiliated Hospital of Guangzhou Medical University for providing the experimental environment.

**Author contributions**

Qianyue Yang, Zhiwei Lin, and Mingshan Xue have contributed equally to this work. Conception and design of the research: Baoqing Sun, Mingshan Xue. Drafting the manuscript: Qianyue Yang and Zhiwei Lin. Article structure design: Qianyue Yang and Zhiwei Lin; Statistical analysis: Qianyue Yang; Samples collection and detection: Libing Chen, Jiahong Chen and Yuhong Liao; Acquisition of data: Jiali Lu and Baojun Guo; Experimental management: Peiyan Zheng, Huimin Huang. All authors read and approved the final version of the manuscript.

**Funding**

Guangdong Zhong Nanshan Medical Foundation (ZNSA-2021005). Guangdong Province Basic and Applied Basic Research Foundation Precision Medicine Joint Foundation (2021B1515230008). Rapid Development and Application of Broad-Spectrum Human Neutralizing Antibodies Against SARS-CoV-2, Zhong Nanshan Medical Foundation of Guangdong Province (2021004). Exploration and Optimization of Early Intervention Strategies and Timing for High-Risk Individuals at Risk of Severe Illness/Death (2022YFC2304803). Enhancing the Treatment and Outcome of COVID-19 Infections through the Use of Medical Consortiums as a Vehicle (ZHYG202339).

**Availability of data and material**

The data that support the findings of this study are available on request from the corresponding authors, upon reasonable request.

**Declarations****Ethics approval and consent to participate**

Informed consent was obtained from all participants, and approval was granted by the Ethics Committee of Guangzhou Medical University Affiliated First Hospital (Ethics Numbers: 202001134 and 202115202).

**Consent for publication**

Not applicable.

**Competing interests**

The authors have declared that no competing interests exist.

**Author details**

<sup>1</sup>Department of Clinical Laboratory, National Center for Respiratory Medicine, National Clinical Research Center for Respiratory Disease, State Key Laboratory of Respiratory Disease, Guangzhou Institute of Respiratory Health, The First Affiliated Hospital of Guangzhou Medical University, Guangzhou 510120, Guangdong, China. <sup>2</sup>Respiratory Mechanics Laboratory, National Center for Respiratory Medicine, Guangzhou Institute of Respiratory Health, First Affiliated Hospital of Guangzhou Medical University, Guangzhou 510120, Guangdong, China. <sup>3</sup>Guangzhou Laboratory, Guangzhou International Bio Island, XingDaoHuanBei Road, Guangzhou 510005, Guangdong Province, China.

Received: 16 November 2023 Accepted: 23 February 2024

Published online: 29 February 2024

**References**

- Kandee M, et al. Omicron variant genome evolution and phylogenetics. *J Med Virol.* 2022;94(4):1627–32.
- Uzun O, et al. COVID-19: vaccination vs. hospitalization. *Infection.* 2022. <https://doi.org/10.1007/s15010-021-01751-1>.
- Dhama K, et al. Global emerging omicron variant of SARS-CoV-2: impacts, challenges and strategies. *J Infect Public Health.* 2023;16(1):4–14.
- He P, et al. SARS-CoV-2 delta and omicron variants evade population antibody response by mutations in a single spike epitope. *Nat Microbiol.* 2022;7(10):1635–49.
- Cao Y, et al. Characterization of the enhanced infectivity and antibody evasion of Omicron BA.2.75. *Cell Host Microbe.* 2022;30(11):1527–39.
- Ramasamy S, Subbian S. Critical determinants of cytokine storm and type I interferon response in COVID-19 pathogenesis. *Clin Microbiol Rev.* 2021. <https://doi.org/10.1128/cmr.00299-20>.

7. Cheung CL, et al. COVID-19 and platelet traits: A bidirectional Mendelian randomization study. *J Med Virol.* 2022;94(10):4735–43.
8. Franco AT, Corken A, Ware J. Platelets at the interface of thrombosis, inflammation, and cancer. *Blood.* 2015;126(5):582–8.
9. Morrell CN, et al. Emerging roles for platelets as immune and inflammatory cells. *Blood.* 2014;123(18):2759–67.
10. Koupenova M, Freedman JE. Platelets and COVID-19: inflammation, hyperactivation and additional questions. *Circ Res.* 2020;127(11):1419–21.
11. Semple JW, Italiano JE Jr, Freedman J. Platelets and the immune continuum. *Nat Rev Immunol.* 2011;11(4):264–74.
12. Sevilya Z, et al. Differential platelet activation through an interaction with spike proteins of different SARS-CoV-2 variants. *J Thromb Thrombolysis.* 2023;56(4):538–47.
13. Zhang S, et al. SARS-CoV-2 binds platelet ACE2 to enhance thrombosis in COVID-19. *J Hematol Oncol.* 2020;13(1):120.
14. Jackson CB, et al. Mechanisms of SARS-CoV-2 entry into cells. *Nat Rev Mol Cell Biol.* 2022;23(1):3–20.
15. Wang H, et al. Multi-omics blood atlas reveals unique features of immune and platelet responses to SARS-CoV-2 omicron breakthrough infection. *Immunity.* 2023;56(6):1410–1428.e8.
16. SB MJ, et al. Biomarkers of coagulation, endothelial, platelet function, and fibrinolysis in patients with COVID-19: a prospective study. *Sci Rep.* 2024;14(1):2011.
17. Bakiera J, et al. Novel inflammatory markers in patients with severe COVID-19 and a pulmonary thrombotic event. *Cent Eur J Immunol.* 2023;48(1):167.
18. Dawson CS, et al. Protein markers for *Candida albicans* EVs include claudin-like Sur7 family proteins. *J Extracell Vesicles.* 2020;9(1):1750810.
19. Ho AM, et al. Label-free proteomics differences in the dorsolateral prefrontal cortex between bipolar disorder patients with and without psychosis. *J Affect Disord.* 2020;270:165–73.
20. Che J, et al. Untargeted serum metabolomics reveals potential biomarkers and metabolic pathways associated with the progression of gastroesophageal cancer. *BMC Cancer.* 2023;23(1):1238.
21. Kupferschmidt K, Vogel G. How bad is Omicron? Some clues are emerging. *Science.* 2021;374(6573):1304–5.
22. Xiang T, Wang J, Zheng X. The humoral and cellular immune evasion of SARS-CoV-2 Omicron and sub-lineages. *Virus Sin.* 2022;37(6):786–95.
23. Jin S, et al. A case of multiple thrombosis and septic shock in a critically ill patient with omicron infection. *J Infect Public Health.* 2022;15(11):1321–5.
24. Wettstein L, et al. Native and activated antithrombin inhibits TMPRSS2 activity and SARS-CoV-2 infection. *J Med Virol.* 2023;95(1):e28124.
25. Zhang H, et al. Epidemiological and clinical features of SARS-CoV-2 omicron variant infection in Quanzhou, Fujian province: a retrospective study. *Sci Rep.* 2023;13(1):22152.
26. Levi M, van der Poll T. Inflammation and coagulation. *Crit Care Med.* 2010;38(2 Suppl):S26–34.
27. Levi M, et al. Infection and inflammation and the coagulation system. *Cardiovasc Res.* 2003;60(1):26–39.
28. Garcia C, et al. SARS-CoV-2 Omicron variant infection affects blood platelets, a comparative analysis with Delta variant. *Front Immunol.* 2023;14:1231576.
29. Krygier A, et al. Molecular pathogenesis of fibrosis, thrombosis and surfactant dysfunction in the lungs of severe COVID-19 patients. *Biomolecules.* 2022;12(12):1845.
30. Shih YT, et al. Vinculin phosphorylation impairs vascular endothelial junctions promoting atherosclerosis. *Eur Heart J.* 2023;44(4):304–18.
31. Grashoff C, et al. Measuring mechanical tension across vinculin reveals regulation of focal adhesion dynamics. *Nature.* 2010;466(7303):263–6.
32. Demali KA. Vinculin—a dynamic regulator of cell adhesion. *Trends Biochem Sci.* 2004;29(11):565–7.
33. Artman L, et al. Planning your every move: the role of  $\beta$ -actin and its post-transcriptional regulation in cell motility. *Semin Cell Dev Biol.* 2014;34:33–43.
34. Jin J, et al. The association between ACTB methylation in peripheral blood and coronary heart disease in a case-control study. *Front Cardiovasc Med.* 2022;9:972566.
35. Wu X, et al. The roles of thrombospondins in hemorrhagic stroke. *Biomed Res Int.* 2017;2017:8403184.
36. Vanhoutte D, et al. Thbs1 induces lethal cardiac atrophy through PERK-ATF4 regulated autophagy. *Nat Commun.* 2021;12(1):3928.
37. Atanasova VS, et al. Thrombospondin-1 is a major activator of TGF- $\beta$  signaling in recessive dystrophic epidermolysis bullosa fibroblasts. *J Invest Dermatol.* 2019;139(7):1497–1505.e5.
38. Sun J, et al. USF2 knockdown downregulates THBS1 to inhibit the TGF- $\beta$  signaling pathway and reduce pyroptosis in sepsis-induced acute kidney injury. *Pharmacol Res.* 2022;176:105962.
39. Vekariya U, et al. Identification of M $\Phi$  specific POTE expression: Its role in mTORC2 activation via protein-protein interaction in TAMs. *Cell Immunol.* 2019;335:30–40.
40. Shen Z, et al. POTE drives colorectal cancer development via regulating SPHK1/p65 signaling. *Cell Death Dis.* 2019;10(11):863.
41. Sjöblom B, Salmazo A, Djinić-Carugo K. Alpha-actinin structure and regulation. *Cell Mol Life Sci.* 2008;65(17):2688–701.
42. Xie GF, et al. High ACTN1 is associated with poor prognosis, and ACTN1 silencing suppresses cell proliferation and metastasis in oral squamous cell carcinoma. *Drug Des Devel Ther.* 2020;14:1717–27.
43. Boutilier JK, et al. Variable cardiac  $\alpha$ -actin (Actc1) expression in early adult skeletal muscle correlates with promoter methylation. *Biochim Biophys Acta Gene Regul Mech.* 2017;1860(10):1025–36.
44. Liu B, et al. Cytoskeleton remodeling mediated by circRNA-YBX1 phase separation suppresses the metastasis of liver cancer. *Proc Natl Acad Sci U S A.* 2023;120(30):e2220296120.
45. Pleines I, et al. Mutations in tropomyosin 4 underlie a rare form of human macrothrombocytopenia. *J Clin Invest.* 2017;127(3):814–29.
46. Gieger C, et al. New gene functions in megakaryopoiesis and platelet formation. *Nature.* 2011;480(7376):201–8.
47. Paluch EK, Aspalter IM, Sixt M. Focal adhesion-independent cell migration. *Annu Rev Cell Dev Biol.* 2016;32:469–90.
48. Mishra YG, Manavathi B. Focal adhesion dynamics in cellular function and disease. *Cell Signal.* 2021;85:110046.
49. Bui TM, Wiesolek HL, Sumagin R. ICAM-1: A master regulator of cellular responses in inflammation, injury resolution, and tumorigenesis. *J Leukoc Biol.* 2020;108(3):787–99.
50. Sumagin R, Lomakina E, Sarelis IH. Leukocyte-endothelial cell interactions are linked to vascular permeability via ICAM-1-mediated signaling. *Am J Physiol Heart Circ Physiol.* 2008;295(3):H969–h977.
51. Cervenka I, Agudelo LZ, Ruas JL. Kynurenines: tryptophan's metabolites in exercise, inflammation, and mental health. *Science.* 2017;357(6349):eaaf9794.
52. Fiore A, Murray PJ. Tryptophan and indole metabolism in immune regulation. *Curr Opin Immunol.* 2021;70:7–14.
53. Prudêncio APA, et al. Red meat intake, indole-3-Acetate, and Dorea longicatena together affect insulin resistance after gastric bypass. *Nutrients.* 2023;15(5):1185.
54. Krishnan S, et al. Gut microbiota-derived tryptophan metabolites modulate inflammatory response in hepatocytes and macrophages. *Cell Rep.* 2018;23(4):1099–111.
55. Rabanal Basalo A, et al. A randomized, double-blind study on the efficacy of oral domperidone versus placebo for reducing SARS-CoV-2 viral load in mild-to-moderate COVID-19 patients in primary health care. *Ann Med.* 2023;55(2):2268535.
56. Lan Y, et al. Upregulation of girdin delays endothelial cell apoptosis via promoting engulfment of platelets. *Mol Biol Rep.* 2023;50(10):8111–20.

## Publisher's Note

Springer Nature remains neutral with regard to jurisdictional claims in published maps and institutional affiliations.